METROLOGY AND MEASUREMENT SYSTEMS
Index 330930, ISSN 0860-8229
www.metrology.pg.gda.pl

INSPECTION OF SPECULAR AND PARTIALLY SPECULAR SURFACES

Stefan Werling[1)], Michael Mai[1)], Michael Heizmann[2)], Jürgen Beyerer[1,2)]

1) Universität Karlsruhe, Institut für Anthropomatik, Lehrstuhl für Interaktive Echtzeitsysteme (IES), Adenauerring 4, D-76131 Karlsruhe, Germany (✉ werling@kit.edu, +49 721 608 5915, mai@kit.edu, beyerer@iitb.fraunhofer.de)
2) Fraunhofer □ Institut für Informations □ und Datenverarbeitung IITB, Fraunhoferstraße 1, D-76131 Karlsruhe, Germany (heizmann@iitb.fraunhofer.de)

Abstract

The inspection of specular surfaces differs significantly from the case of non-specular surfaces. In contrast to the non-specular case, the appearance of a specular surface is dominated by the reflections of the environment that are visible in it. The transfer of this observation into automated visual inspection is called deflectometry. The main principle of deflectometric surface acquisition is to use a highly controllable environment, where a screen on which a well-defined pattern is presented is observed via the specular reflecting surface. Knowing that pattern, it is possible to inspect the surface qualitatively and □ at least with certain additional knowledge □ to reconstruct the surface under test. In this paper, we introduce the theoretical background of deflectometry. After presenting some properties of the deflectometric inspection itself, we describe the qualitative and quantitative evaluation of the deflectometric observation in detail. We will show that an inspection of specular and partially specular objects is feasible in an industrially applicable inspection system. For complexly formed and/or large objects, we propose a robot-based inspection setup.

Keywords: shape from Specular Reflection, deflectometry, specular surface, reconstruction, regularization, robot based inspection.

1. Introduction

Let us consider our knowledge about object surfaces from a technical and visual perspective. There are two aspects we can distinguish: the reflectance and the shape.

Once the bidirectional reflectance distribution function (BRDF) for every point of the surface is known, all information about the reflectance properties of the surface is available [1]. The BRDF as a function of the geometric arrangements of the illumination and the observation relative to the surface normal describes how bright the surface will appear in proportion to a given irradiance. Many types of automated visual inspection methods for industrial surfaces use the knowledge of the BRDF implicitly. The evaluation of spectral properties of the surface, which determine its visible color, can be interpreted as a special case of the application of the BRDF, which then comprises the wavelength as an additional argument.

Other surface properties that can be evaluated are geometric properties, which ultimately describe the object shape. Knowledge about this aspect is usually represented through an object model. The simplest form of such a model is a 3D point cloud, which is usually the raw data obtained directly through a measurement process that supplies the position of measurement points. The problem of finding a more appropriate model for given raw data is one of the fundamental problems for the reconstruction of 3D objects in computer graphics [2, 3]. In the context of industrial automated visual inspection systems, we can stress at least two inspection tasks considering object shape-first: how well fits the global geometry of the object under test fits into its designed shape, and second: is there a local object deformation.

How do these aspects appear in the context of the present inspection task, the inspection of specular and complex surfaces? The at least partially specular nature of the objects under test implies the validity of the law of geometric optic reflection. This knowledge is the only precondition we will take into account. Hence, for specular surfaces, the BRDF is well known. For partially specular surfaces, it is possible to model the reflection through a specular and a diffuse component. For many types of practically relevant surfaces, it is sufficient for automated visual inspection to employ the well known Phong shading model, which assumes a perfectly diffuse reflection component and a specular component that decays polynomially from the ideal specular direction [4]. In either case, it is assumed that it is possible to determine the direction of the specular reflection.

For the surface reconstruction problem, we will assume that the reflectance properties of the objects under test are known and focus on the determination of the object shape. The main challenge in the field of automated visual inspection of specular surfaces can be stated as follows: how can we gather information about a surface only by assuming its specular property? In the field of computer graphics, this problem is known as shape from specular reflection or shape from specularities, whereas in the metrology community the terms deflectometry and reflection grating method are more prevalent. Early work in the field of estimating surface deviations using lighting reflection techniques were done by Kafri and Livnat [5], Ikeuchi [6], and Ritter and Hahn [7]. Ikeuchi and later Sanderson *et al*. [8] used the basic deflectometric principle, which can be described as follows: a presumably distorted (deflected) image of a well known and calibrated scene or light source is captured with an image acquisition device such that the light path includes the unknown specular surface. Knowing the intrinsic and extrinsic parameters of the camera, the light source and the image acquisition constellation, it is possible to obtain normals of the unknown surface. The mapping from sight ray to scene point the deflectometric measurement is usually done by a definite coding of the scene positions. It is well known that the surface reconstruction problem for such a simple setup is mathematically ill-posed.

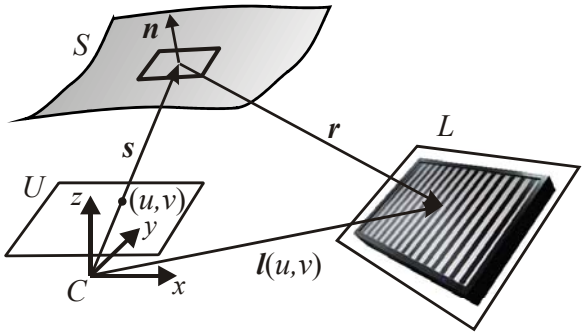

Fig. 1. General geometric setup for deflectometric inspection.

For a deeper understanding of the mathematical background of the deflectometric regularization problem, we refer the reader to the work of Balzer [9].

This contribution is organized as follows: in Section 2, we give a short introduction into the geometric setup of deflectometric image acquisition. Section 3 highlights important properties of the deflectometric optical path that determine a sensible inspection setup. The evaluation of deflectometric observations is the topic of Section 4. Section 5 describes a compact sensor as a part of a robot based inspection system for the inspection of large industrial parts.

2. Foundations of Deflectometry

The general geometric setup is depicted in Fig. 1. We employ a central perspective camera model with projection center C and camera coordinates (u, v) lying in a projective plane. A pattern sequence presented on a pattern generator, *e.g.* a liquid crystal display, constitutes the light source L. The pattern sequence is a realization of a spatial coding *e.g.* phase shifting or Gray code that is needed to identify each pixel on the pattern generator. The origin and the orientation of the display coordinate system relative to the camera system are known due to a calibration process. Deflectometric measurement means then recording the assigned display position l (u, v) for each camera pixel (u, v).

3. Properties of the Deflectometric Inspection

In comparison to other optical inspection principles, deflectometry shows a significantly different dependence on specific imaging parameters. These relations can be used to vary the sensitivity of a deflectometric setup in order to find an optimal sensor configuration for a given inspection task. There are two major parameters whose effects differ significantly from other optical inspection principles, *e.g.* projection methods:

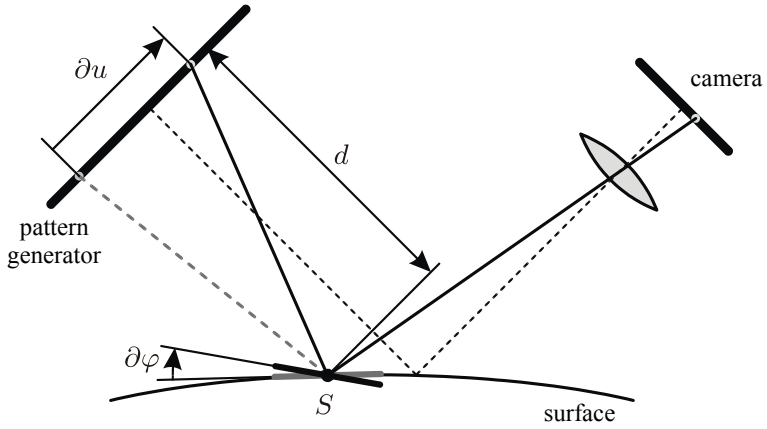

Fig. 2. Angular resolution.

First, the distance of the pattern generator to the surface determines the sensitivity to inclination changes in the surface (*i.e.* the angular resolution), the range of determinable inclinations and the measuring field on the surface. The relation between the sensitivity to inclinations $\partial u / \partial \varphi$ and the distance d (see Fig. 2) can be approximated by the proportionality:

$$\frac{\partial u}{\partial \varphi} \propto d \ .$$

Thus, in theory, any given angular resolution is obtainable by moving a pattern generator with fixed pixel spacing sufficiently far away from the surface. However, by doing so, the range of determinable inclinations $R(\varphi)$ is reduced by $R(\varphi) \propto 1/d$ since the pattern generator covers a smaller angle that is visible from a certain surface point S. In addition, if a flat surface is considered, the measuring field on the surface MF becomes also reduced by $MF \propto 1/d$ In consequence, given a certain pattern generator, there exists always a tradeoff between (1) the angular resolution and (2) the range of determinable inclinations and the measuring field. If a large range of determinable inclinations is mandatory, the use of a

spherical pattern generator, *e.g.* by projecting a pattern on a spherical screen, is a possible solution [10]. A high angular resolution together with a large measuring field is obtainable by dividing the surface of interest into several measuring fields which can be inspected individually. Such an approach can be realized by means of a deflectometric sensing head consisting of a pattern generator and one or several cameras, which is mounted on an industrial robot, see Section 5.

A second degree of freedom in the deflectometric image acquisition is the focus adjustment of the camera lens. Whereas for most other optical measuring principles, focusing mainly influences the lateral resolution on the surface, focusing in the deflectometric inspection additionally influences the angular resolution. In this context, two particular focus settings can be identified:

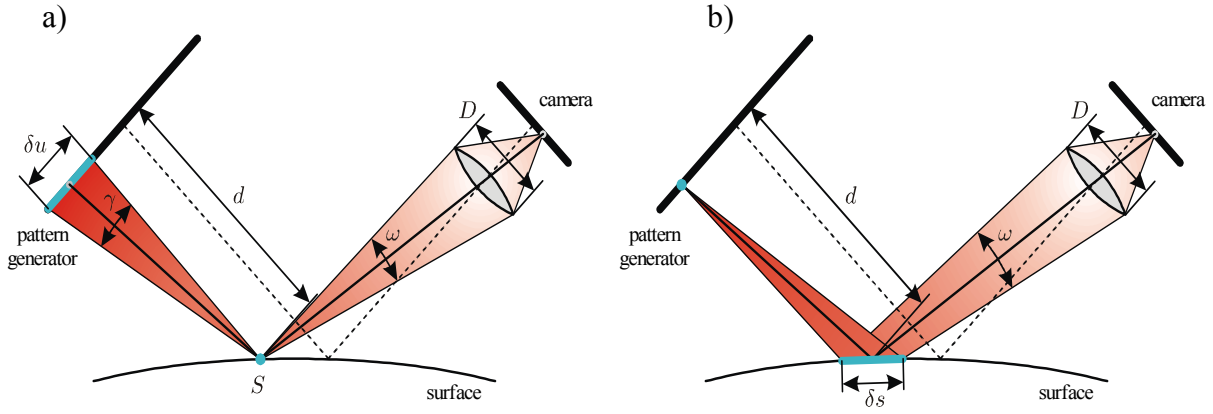

Fig. 3. Focus settings: a) focusing on the surface, b) focusing on the pattern generator.

When the camera focuses on the surface, optimal lateral resolution on the surface can be obtained, see Fig. 3a. If a flat surface in the vicinity of the actual inspection point S is considered, the aperture angle of the camera ω effects that the observed intensity at S is obtained by integrating the visible radiance over γ with $\gamma = \omega$, which leads to a blurred imaging of the pattern generator. In a system theoretic point of view, the blurring can be approximated by the substitution of the originally displayed pattern $l(u)$ for the convolution $l_b(u) = l(u) * b(u)$ with $b(u) = (\delta u)$, where δu is the size of the area that is visible on the pattern generator due to the integration over γ. In consequence, if the surface is to be focused to obtain the optimal lateral resolution, a coding with low-frequency patterns has to be chosen that is insensitive to blurring. Such patterns are *e.g.* sinus patterns that are commonly used for phase shifting methods. Other codings such as Gray codes have high frequency components which are deteriorated by the blurring.

When the camera is focused on the pattern generator, the pattern on the screen can be identified without blurring, such that the angular resolution becomes optimal, see Fig. 3b. However, the aperture angle of the camera ω causes the integration of the reflected light over the area δs on the surface, leading to a reduced lateral resolution. The curvature of the surface acts as an additional optical component in the deflectometric optical path. Hence, a necessary precondition focusing between the surface and the pattern generator. The suitable focus setting has to be chosen such that an optimum between high lateral resolution on the one hand and high angular resolution on the other for perfect focusing on a flat screen in the entire camera image is that the curvature of the surface is constant over the visible area. Since real surfaces often satisfy this condition only in small regions and certainly not in defective areas, a focus setting leading to an overall focused imaging of the pattern generator does generally

not exist. An optimal focus setting can be obtained *e.g.* by raytracing, when the pattern generator is fitted into a set of simulated points leading to a focused imaging for many surface points [10].

A good compromise for the focus setting can be obtained by hand is reached. The effects of different focus settings can be reduced by stopping down the camera optics, leading to a reduction of the aperture D and in consequence of the angles ω and γ.

4. Evaluation of Deflectometric Observations

Deflectometric observations can be evaluated in different ways, the choice of which depends on the purpose of the surface inspection. A common approach is to extract local features from the patterns observed in the specular surface [11]. This approach offers the advantage of a fast inspection and will be presented in Section 4.1.

A second approach is to reconstruct the surface from the deflectometric observations such that the geometry of the surface is quantitatively accessible, see Section 4.4. However, it is well known that the quantitative reconstruction requires additional information on the surface. Once such additional information is available, the major drawback of this approach is its computational expense.

4.1. Pattern Recognition for the Evaluation of Deflectometric Observations

Suitable features are the basis for methods of pattern recognition. In case that the geometric properties of the surface are of interest, the analysis is best performed directly on geometric data. Normal fields that will be introduced in Section 4.4 are predestinated as features for this task.

Deflectometric observations can also be applied for the analysis of reflectance properties of partially specular surfaces. For this task, the total reflected radiance can be taken as a feature. If a suitable code sequence is displayed on the pattern generator, the summarized Gray values over the image series at a certain image point represent an adequate realization. In case that the color of the surface is of interest, the color in the received images of a partially specular surface depends on the surface reflection and in addition on the body reflection [12]. Only the body reflection affects a possible color shift and can be used *e.g.* for characterizing the material of the surface.

Some tasks require the combination of the evaluation result with additional information. The consideration of “customer acceptance” is a kind of additional information. As an example, the perceptibility the visibility according to physical and physiological limits and the relevance may come into play. For surfaces which have to be inspected for aesthetical defects, the question is important whether a defect is located at a position where the customer imposes aesthetical requirements or not [13]. However, the quantitative assessment of the relevance of aesthetical defects is still an open problem. In case of technical surfaces, the location of a possible functional defect is important in a similar way.

4.2. Analysis of Homogeneity

A possible way of analyzing deflectometric features is to consider their homogeneity. For many practically important surfaces, geometric or reflectance features at a certain surface point must not significantly differ from its surrounding area. Another approach is to check the features against a predefined sample.

To evaluate the homogeneity of features, many techniques have been developed in different scientific fields. As examples, the following methods exploit different concepts:

- **Auto-regressive models (ARMs):** ARMs base on the prediction of the feature value at a certain image point by a linear combination of the values in a neighboring area [14, 15]. They perform an optimal linear prediction in a least-squares sense based on a statistical analysis in a learning region. The obtained parameters of the ARM can be interpreted as texture features for the learning region. If an inhomogeneity is present, the prediction error rises significantly and can be used to detect inhomogeneities. Benefits of ARMs are their well-founded theory and the computational simplicity in comparison to other methods.
- **Local binary patterns (LBPs):** LBPs perform a direct comparison of the feature values at neighboring image points [16]. They exploit the idea that the sign of feature differences in several directions contains enough information to assess homogeneity. Due to this simple assumption, LBPs are easily parameterized, fast and surprisingly successful.
- **Co-occurrence matrices:** They determine local feature similarity through the statistical evaluation of feature values at certain displacements within small neighboring areas. A subsequent analysis of the resulting second-order statistics *e.g.* by means of the Haralick-features extracts texture descriptors that can be used to assess homogeneity [17].

For each class of methods, reference feature vectors must be predefined. After the deflectometric image data has been processed, the concept of feature distance must be applied in order to decide whether the measured features are close enough to the reference feature vector *i.e.*, homogeneity is assumed or not. The definition of a feature distance must ensure that it allows for tolerable variations in the image acquisition, *e.g.* illumination conditions that may vary between the recording of the sample and the actual surface to be inspected. It depends on the application whether the distance should base on the Euclidean or any other metric.

A commonly used non-Euclidean metric is the radial base function (RBF) metric. It assumes that the feature vectors that are closer to the vector of interest should have a greater influence than more distant ones. In this way, it is possible to adjust how important local clusters of feature values are. RBF metrics are often used in support vector machines as RBF Kernels.

Even very customized metrics can be used. As an example, the closest feature values together with the most distant ones could be ignored, while the ones in between are considered. This behavior would be comparable to a band-pass filter that only includes certain parts of the spectrum.

4.3. Pattern Recognition for Geometric Features

As mentioned above, normal fields (see Section 4.4) which constitute the immediate result of a deflectometric inspection are suitable as natural geometric features for pattern recognition. If necessary, even a quantitative reconstruction of the geometry of the surface can be sensible as the basis for the pattern recognition. However, this approach implies a high complexity and high computational costs. Nevertheless, the reconstruction is the most meaningful representation of a 3D surface.

To circumvent the problem of reconstruction, a possible solution could be to use a coarse model assumption of all normal vectors and to use an approximated inclination and the resulting curvature as geometric features.

If we are only interested in the local topological or geometric differentials which are sufficient for many pattern matching tasks it is suitable to work on normal fields or their derivatives (*e.g.* the relative inclination and the curvature) themselves. For this comparison, the reference pattern has to be transformed into a field of relative inclination curvature. The resulting matching is then done with rotation-invariant techniques such as spin images [18].

4.4. The Deflectometric Reconstruction Problem

Because of the precondition that the reflection law holds for each surface point, the following relation between the sight ray $\boldsymbol{s}$ to the surface S, the reflected ray $\boldsymbol{r}$, and the local surface normal $\boldsymbol{n}$ holds (vectors of unit length are marked by an additional hat, *i.e.* $\|\hat{\boldsymbol{x}}\| = 1$):

$$\boldsymbol{n} = \frac{\boldsymbol{s}}{\|\boldsymbol{s}\|} - \frac{\boldsymbol{r}}{\|\boldsymbol{r}\|} = \hat{\boldsymbol{s}} - \hat{\boldsymbol{r}} \,. \tag{1}$$

From this equation follows with $\boldsymbol{r} = \boldsymbol{l} - \boldsymbol{s}$ (see Fig. 1) the relation between possible surface normals $\boldsymbol{n}_{\mathrm{m}}$ due to the measurement and the measurement $\boldsymbol{l}(\boldsymbol{u})$ itself, with $\boldsymbol{u} \in U \subset \mathbb{R}^2$ for all $\boldsymbol{x} \in \Omega$ with $\Omega = \{\boldsymbol{x} \mid \boldsymbol{x} \in \mathbb{R}^3 \wedge \boldsymbol{P}(\boldsymbol{x}) \subseteq U\}$:

$$\boldsymbol{n}_{\mathrm{m}}(\boldsymbol{x}) = \hat{\boldsymbol{x}} - \widehat{\boldsymbol{l} - \boldsymbol{x}} = \frac{\boldsymbol{x}}{\|\boldsymbol{x}\|} - \frac{\boldsymbol{l}(\boldsymbol{P}(\boldsymbol{x})) - \boldsymbol{x}}{\|\boldsymbol{l}(\boldsymbol{P}(\boldsymbol{x})) - \boldsymbol{x}\|} =: \boldsymbol{m}(\boldsymbol{x}, \boldsymbol{l}(\boldsymbol{P}(\boldsymbol{x}))) \,. \tag{2}$$

Here $\boldsymbol{P} : \mathbb{R}^3 \to \mathbb{R}^2$ denotes the projection $\boldsymbol{P}(\boldsymbol{x}) := (x_1 / x_3, x_2 / x_3)^{\mathrm{T}}$, $\boldsymbol{x} = (x_1, x_2, x_3)^{\mathrm{T}}$.

Note that for all $\boldsymbol{x} \in S$ and undisturbed measurement,

$$\hat{\boldsymbol{n}}(\boldsymbol{x}) = \boldsymbol{n}_{\mathrm{m}}(\boldsymbol{x}) \tag{3}$$

must hold. For all $\tilde{\boldsymbol{x}} \in \Omega - S$, $\hat{\boldsymbol{n}}_{\mathrm{m}}(\tilde{\boldsymbol{x}})$ is a possible surface normal to a hypothetical surface $\tilde{S}$ in the sense that $\tilde{S}$ would lead to the same deflectometric measurement $\boldsymbol{l}(\boldsymbol{u})$ as S.

We can summarize: the deflectometric measurement establishes a normal field $\hat{\boldsymbol{n}}_{\mathrm{m}}(\boldsymbol{x})$ so that the deflectometric reconstruction problem reads as: find the very surface which fits into this measured normal field.

4.5. The Reconstruction Problem for Parameterized Surfaces

The surface S can be described in local camera coordinates as the graph of a function f using the following parametrization:

$$S = \{(x, y, z)^{\mathrm{T}} \mid z = f(x, y)\}, \quad \hat{\boldsymbol{n}} = \frac{1}{\sqrt{(\partial_x f)^2 + (\partial_y f)^2 + 1}} \begin{pmatrix} -\partial_x f \\ -\partial_y f \\ 1 \end{pmatrix}. \tag{4}$$

For each surface point Eq. (3) must hold. This leads to the following nonlinear deflectometric PDE:

$$-\nabla f(x, y) = \begin{pmatrix} \hat{n}_{\mathrm{m},1} / \hat{n}_{\mathrm{m},3} \\ \hat{n}_{\mathrm{m},2} / \hat{n}_{\mathrm{m},3} \end{pmatrix} =: \boldsymbol{q}(x, y, f) = \begin{pmatrix} q_1(x, y, f(x, y)) \\ q_2(x, y, f(x, y)) \end{pmatrix}. \tag{5}$$

Many deflectometric reconstruction approaches use a linear variant of this equation, see *e. g.* Massig [19], which implicitly implies some regularization process selecting the *correct* normals $\hat{\boldsymbol{n}}_{\mathrm{s}}$ to the real surface out of the normal field $\hat{\boldsymbol{n}}_{\mathrm{m}}$ (cf. Section 4.7):

$$(x, y)^{\mathrm{T}} \mapsto \hat{\boldsymbol{n}}_{\mathrm{s}}, \quad \mathbb{R}^2 \to \mathbb{R}^3, \quad \hat{\boldsymbol{n}}_{\mathrm{s}}(x_0, y_0) \in \{\hat{\boldsymbol{n}}_{\mathrm{m}}(x, y, z) \mid x = x_0, y = y_0\} \,. \tag{6}$$

With the surface representation of Eq. (4), this mapping yields the linear variant of problem (5):

$$-\nabla f(x,y) = \hat{\boldsymbol{q}}(x,y)\,. \tag{7}$$

Hereby we have to point out that first selecting the normals $\hat{\boldsymbol{n}}_s$ is not sufficient to reconstruct the unknown surface, since we need initial and/or border values to solve the reconstruction problem [20], and that second the normal field is not necessarily curl free, which implies that a potential f might not exist and only an approximative solution can be achieved.

Many approaches exist in literature for normal field integration, directly or implicitly using Eq. (7), *e. g.* Frankot and Chellappa [21] have shown that a surface projection onto an integrable subspace can be reconstructed by applying Fourier transform techniques. This solves the problem of possible non-integrable normal fields, but introduces the problem of the inherently periodical surface continuation due to the Fourier transform. Terzopoulos [22] uses a variational approach to the reconstruction problem by minimizing an energy functional containing terms for position and normal deviation. Karaçali and Snyder [23, 24] describe an adaptive surface reconstruction method from a normal field that allows discontinuities in the solution and a gradient space technique for noise reduction of disturbed normal fields. Kickingereder and Donner [25] introduce a method for the simultaneous normal selection and integration procedure based on a stereo approach and applying B-splines as surface model. Ettl *et al.* [26, 27] use a fitting method using B-splines for approximating the derivatives of the surface shape and radial basis functions (RBF) for the deflectometric surface approximation problem.

Another solution approach for the reconstruction problem is opened by looking at the norm of ∇f , which leads directly from Eq. (7) to the following eikonal equation:

$$\left\|\nabla f(x,y)\right\| = \sqrt{{q_1}^2 + {q_2}^2}\,, \tag{8}$$

which can be solved by applying the Fast Marching Method, cf. Ho *et al*. [28].

Kovesi [29] uses a wavelet approach (applying so-called shapelets) for the shape recovery problem, which can even deal with an ambiguity in the measured surface tilt of π.

Furthermore it is possible to directly utilize the nonlinear problem (5), which can be transformed into a scalar PDE by applying the divergence operator:

$$-\Delta f(x,y) = \operatorname{div} \boldsymbol{q}(x,y,f)\,. \tag{9}$$

From the theory of partial differential equations it is well known that a variational formulation for this problem exists [30], which allows weak solutions.

In the following, we will emphasize on the reconstruction problem using implicit surface models.

4.6. The Reconstruction Problem for Implicit Surfaces

This chapter is substantially based on the work of Balzer [9].

Balzer has shown that the solution space of the deflectometric reconstruction problem is a one-dimensional manifold. As mentioned before, this means that there exists an infinite number of hypothetical surfaces S_c which could have lead to the same deflectometric measurement. These surfaces can be modeled by a family of level sets of an implicit surface representation:

$$S_c = \{\boldsymbol{x} \mid \varphi(\boldsymbol{x}) = c,\ \boldsymbol{x} \in \Omega \subset \mathbb{R}^3,\ c \in \Xi \subset \mathbb{R}\},\quad \boldsymbol{n}(\boldsymbol{x}) = \nabla\varphi(\boldsymbol{x}),\quad \Omega = \bigcup_c S_c\,. \tag{10}$$

This means that we are looking for a level set function φ which simultaneously describes all solutions of the reconstruction problem in the volume Ω. Therefore, the normal adaption condition (3) must hold for any point $\boldsymbol{x} \in \Omega$, which means that the normal directions to the level sets must fit the normal directions induced by the measurement (note that the deflectometric measurement yields only information about normal directions):

$$\frac{\nabla \varphi}{\|\nabla \varphi\|} = \hat{\boldsymbol{n}}_{\mathrm{m}} . \tag{11}$$

Allowing slightly disturbed measurements to reduce this rigid condition, a variational approach is convenient:

$$J[\varphi] := \frac{1}{2} \int_{\Omega} \left\| \frac{\nabla \varphi}{\|\nabla \varphi\|} - \hat{\boldsymbol{n}}_{\mathrm{m}} \right\|^2 d\boldsymbol{x} \to \min . \tag{12}$$

Clearly, for an undisturbed measurement, this energy functional will reach zero as its minimum. To eliminate the norm term $\|\nabla \varphi\|$, an implicit, soft constraint $\|\nabla \varphi\| = 1$ can be introduced, leading to the following minimization problem:

$$E[\varphi] := \frac{1}{2} \int_{\Omega} \|\nabla \varphi - \hat{\boldsymbol{n}}_{\mathrm{m}}\|^2 d\boldsymbol{x} \to \min . \tag{13}$$

A necessary condition for a minimum of $E[\varphi]$ is:

$$\frac{\partial}{\partial \varepsilon} E[\varphi_\varepsilon]\big|_{\varepsilon=0} = 0 , \tag{14}$$

denoting the variation of φ as $\varphi_\varepsilon = \varphi + \varepsilon \eta$ with $\varepsilon \in \mathbb{R}$ and $\eta \in C_0^2(\mathbb{R}^3)$. Inserting this variation in Eq. (13) and applying the condition of Eq. (14) yields:

$$\frac{d}{d\varepsilon} E[\varphi_\varepsilon]\Big|_{\varepsilon=0} = \frac{1}{2} \int_{\Omega} \frac{d}{d\varepsilon}\Big|_{\varepsilon=0} \|\nabla(\varphi + \varepsilon\eta) - \hat{\boldsymbol{n}}_{\mathrm{m}}\|^2 d\boldsymbol{x} . \tag{15}$$

Execution of the derivation and using partial integration and Gauss' theorem leads to:

$$\int_{\partial\Omega} \langle \nabla \varphi - \hat{\boldsymbol{n}}_{\mathrm{m}}, \hat{\boldsymbol{o}} \rangle \eta \, d\boldsymbol{x} - \int_{\Omega} \operatorname{div}(\nabla \varphi - \hat{\boldsymbol{n}}_{\mathrm{m}}) \eta \, d\boldsymbol{x} = 0 \tag{16}$$

with $\hat{\boldsymbol{o}}$ denoting the outer normal to $\partial\Omega$. From the second summand, the Euler-Lagrange equation follows for the deflectometric reconstruction problem:

$$\Delta \varphi = \operatorname{div} \hat{\boldsymbol{n}}_{\mathrm{m}} , \tag{17}$$

whereas the first summand leads to a Neumann problem with natural boundary condition:

$$\langle \nabla \varphi, \hat{\boldsymbol{o}} \rangle = \langle \hat{\boldsymbol{n}}_{\mathrm{m}}, \hat{\boldsymbol{o}} \rangle \tag{18}$$

on $\partial\Omega$. Solving this linear problem yields an approximative reconstruction for all possible surfaces in Ω. The natural boundary conditions can easily be fulfilled, because the normal directions on the boundary are known by measurement. To select the real surface out of the solution manifold, that is selecting a level of φ, additional information is needed (note that with $\varphi(\boldsymbol{x}) = 0$, also $\varphi(\boldsymbol{x}) + k = 0,\ k \in \mathbb{R}$ is a solution of Eqs. (17), (18)).

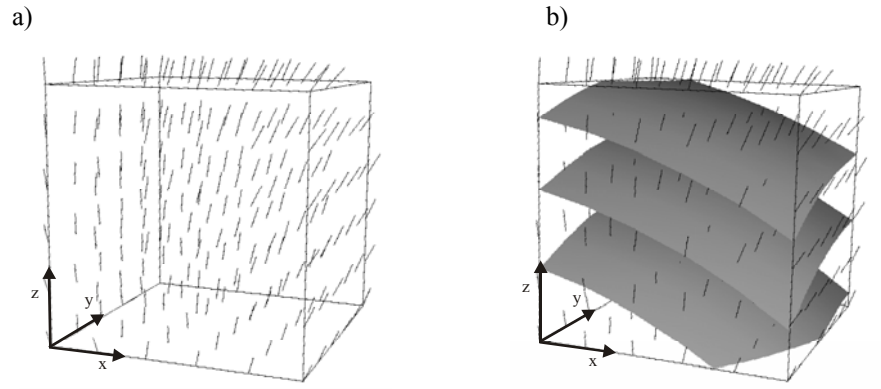

Fig. 4. Example of a normal field a) and some reconstructed surfaces b) all solving the problem of Eq. (17).

4.7. Regularization

From each formulation of the deflectometric problem (Eqs. (5), (7), (8), and (17)) follows that initial and/or boundary values must be given to solve the particular system of differential equations. In other words: with a given setup consisting of a camera and a pattern generator, it is impossible to solve the reconstruction problem without additional information. The situation is visualized in the example of Fig. 4, where an infinite number of surfaces fit into the measured normal field. Consequently, the problem has to be regularized.

There are a number of regularization methods proposed in literature for the deflectometric reconstruction problem:

- **A priori model knowledge**: Knowing the underlying surface model of the object under test, it is possible to estimate the unknown model parameters. The reconstruction problem becomes a problem of parameter estimation [31]. The evaluation of the local connectivity of the images of known scene curves delivers a set of equations for the local surface reconstruction. Our experiments have shown that, generally speaking, the fitting of a known surface to a normal field is numerically ill-conditioned.
- **Optical Flow**: With an infinitesimal translation of the surface, the correspondence problem of mapping the sight ray to a surface point is manageable. Evaluating the optical flow delivers the necessary additional information for the reconstruction problem. Zisserman *et al.* [32] brought up the idea of using observer movement to gather information about specular surfaces. Roth and Black [33] introduced optical flow resulting from known displacement fields in the specular surface reconstruction process. Their approximative model was enhanced by Lellmann *et al*. [34] where a set of closed-form analytical equations was derived.
- **Polarisation**: This approach is based on a priori knowledge about the angular dependency of the polarization state on the directions of the illumination and the observation for a given surface. That way, it is possible to gather information about surface normals by evaluating a polarization series. This information can be applied in the regularization process. A polarization-based technique for calculating normals for specular surfaces was introduced by Rahmann and Canterakis [35]. A reconstruction technique for diffusely reflecting surfaces was proposed by Wolff [36]. Atkinson [37] gives a good survey of the connection between surface shape and polarization.

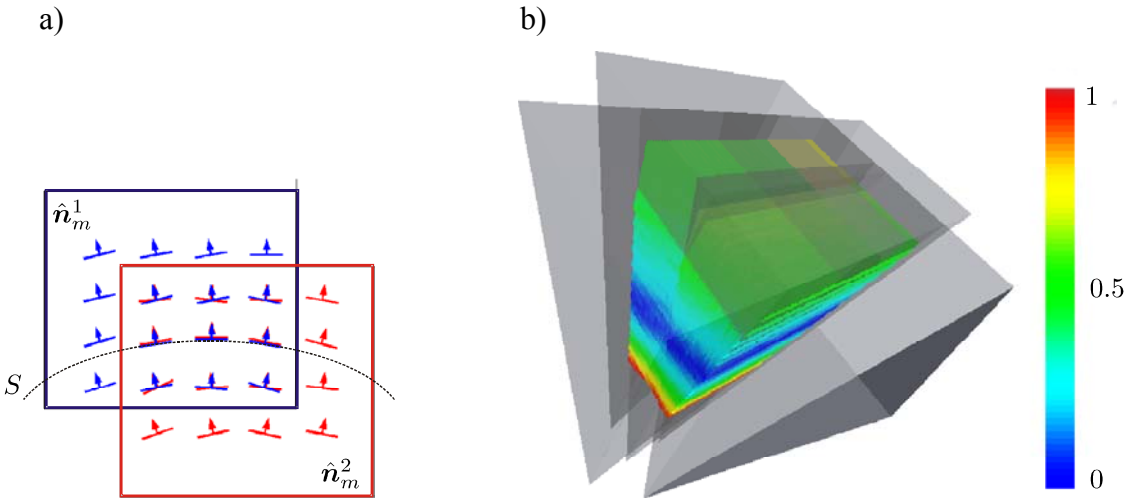

Fig. 5. Disparity of normal fields from a stereo approach: a) normal fields for two measurement patches in 2D, b) measurement disparity field for five overlapping measurements volumes with color coded disparity $d(\boldsymbol{x})$.

– **(Multi) Stereo**: Stereo methods for specular surface reconstruction could be considered as the traditional approach. The idea of using multiple views to gather information about surfaces and their normals has been adopted early by Ikeuchi [6]. Later on, Wang and Inokuschi [38], Bonfort *et al*. [39], Knauer *et al*. [40], Kickingereder and Donner [25] and Petz and Tutsch [41], among others, picked up this approach successfully.

  A deflectometric measurement with a single camera setup yields a normal field $\hat{\boldsymbol{n}}_{\mathrm{m}}{}^{1}$ in the considered measuring volume, cf. Eq. (2). For a different camera view, a second measurement with associated normal field $\hat{\boldsymbol{n}}_{\mathrm{m}}{}^{2}$ is obtained. Points in space for which the attached normals match closely are possible surface points. In this case the disparity of the normals is minimal. A simple disparity measure is the length of the difference vector $d(\boldsymbol{x}) = \left\| \hat{\boldsymbol{n}}_{\mathrm{m}}{}^{1}(\boldsymbol{x}) - \hat{\boldsymbol{n}}_{\mathrm{m}}{}^{2}(\boldsymbol{x}) \right\|$ of the unit normals. A more elaborate measure was introduced by Bonfort and Sturm [39] especially for multi stereo approaches.

  Fig. 5 illustrates this idea. The left figures shows two overlapping normal fields in a 2D view. Points where both normals have the same direction indicate the real surface which has generated the normal fields. The right figure shows the disparity field $d(\boldsymbol{x})$ for five overlapping measurement volumes obtained with a deflectometric sensor head at different positions. The area with nearly zero disparity indicates real surface points. An algorithm for the determination of regularization values from such a monocular stereo setup has been presented by the authors [20]. Estimating surface normals only in boundary regions by monocular stereo, allows surface reconstruction by solving a boundary value problem.

  Stereo methods cannot be used only for the estimation of initial values, but also for the estimation of normal fields and/or surface points (cf. Eq. (6)).

  Although stereo approaches are commonly used, a serious drawback has to be mentioned: for general surfaces, the determination of the minimal disparity and therefore of surface points and normals is difficult and ambiguous [42], this holds especially for surfaces with concavities.

– **Shape From Shading (SFS)**: The SFS problem is, with respect to some important properties, analogous to the deflectometric reconstruction. Both, SFS and *Shape From Specular Reflection*, yield information about surface normals. Therefore, it is possible to gather the necessary additional information by illuminating a partially specular surface

with directional light and by evaluating its diffuse reflection with SFS [43]. It is obvious that this regularization method works only for partially specular surfaces.

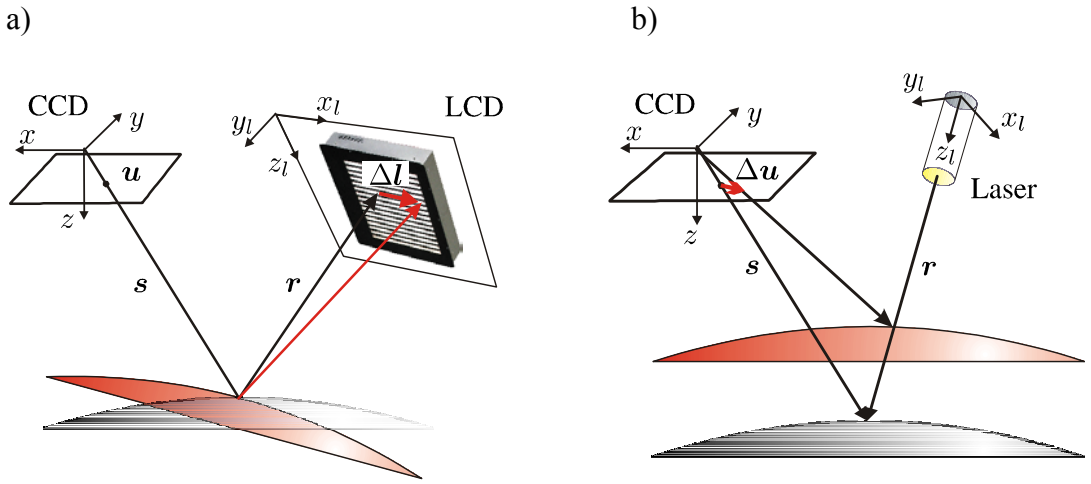

Fig. 6. Sensitivity of deflectometric a) and triangulation based methods b).

– **(Laser) Triangulation**: This is another regularization method which is like the SFS approach only applicable for partially specular surfaces. Due to the fact that the solution space of the deflectometric problem is one-dimensional, the additional estimation of the position of only one surface point is sufficient for solving the reconstruction problem. With triangulation based methods, it is possible to determine such a point with high accuracy. Furthermore, these methods are complementary to deflectometry in the sense of delivering zero-order surface information □ the positions of points themselves □ instead of first-order information □ *i.e.* the inclination □ in the deflectometric case, see Fig. 6. In the case of deflectometry (Fig. 6a), a local inclination change yields a different measurement $\Delta \boldsymbol{l}(u,v)$ for a fixed sight ray, whereas in the triangulation case (Fig. 6b), a local change of the surface height leads to a different sight ray $\Delta \boldsymbol{u}$, which is directly proportional to height changes.

If the object under test is partially specular, we would strongly recommend this approach because of its robustness and the uniqueness of its result.

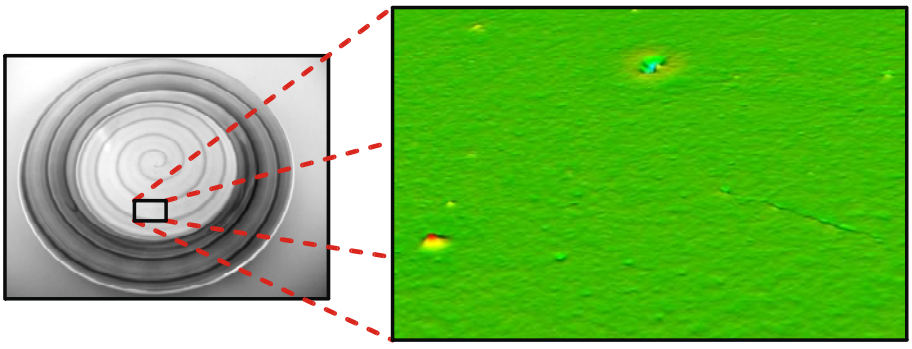

Fig. 7. Reconstruction of ceramic glaze defects at dishes.

12. Surface Reconstruction

For the industrially relevant tasks reconstructing the global shape of a specular object and detecting local deformations we use a formulation of the deflectometric problem in the form of differential equations, cf. Eq. (5), (7), and (17). In the following, we will present some aspects of using the Poisson equation Eq. (17) and natural boundary values Eq. (18). The first detail to recapitulate is the three-dimensionality of the problem formulation. The one-dimensional solution manifold is obtained simultaneously. Selecting a solution in this case means to regularize the problem, which is done either by monocular stereo several positions of a deflectometric sensor head, see Section 5 or by laser triangulation as described above. An example for a deflectometric surface reconstruction is depicted in Fig. 7, where small defects on the glaze of the dish are clearly detectable. An important advantage of having multiple solutions in overlapping volumes at hand is the possibility to fuse neighboring surface patches, see Fig. 8. In the context of a robot-based inspection system, this allows for the reconstruction of complexly shaped specular objects, which commonly requires deflectometric measurements from several different directions.

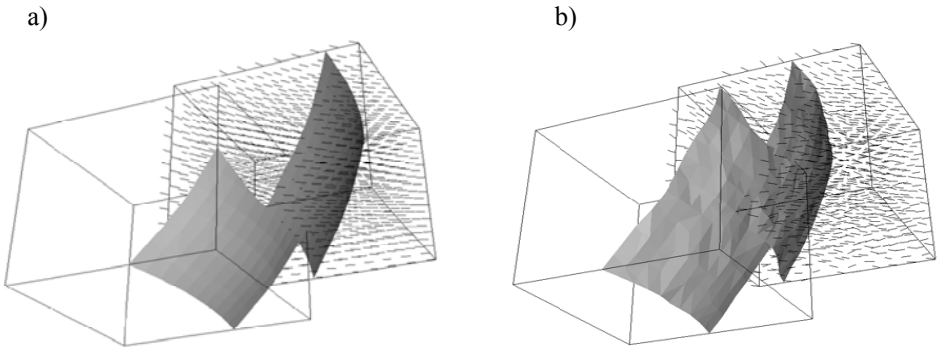

Fig. 8. Reconstruction and fusion of two overlapping surface patches: a) reconstruction on the basis of undisturbed normal fields, b) reconstruction on the basis of normal fields that are heavily disturbed with equally disturbed random changes of normal directions in the range of 20°.

For the numerical solution of the Poisson equation, we employ finite element methods (FEM). Thereby, the Galerkin projection is used, which leads to an implicit smoothing of the solution and results in high robustness regarding normal field distortions. Another advantage of FEM is the possibility to automatically generate locally refined meshes, either for the reconstruction of local shape variations or for speeding up calculations by using adaptive mesh refinements, see Fig. 9.

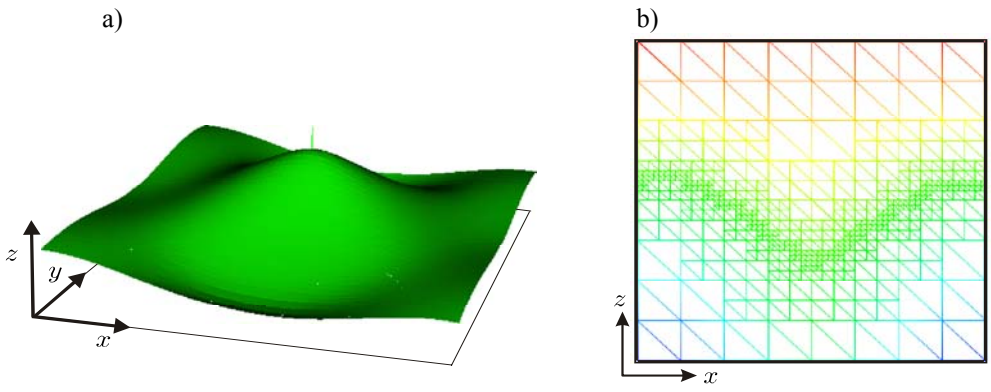

Fig. 9. Adaptive surface reconstruction with finite element methods: a) final reconstruction, b) adaptive mesh refinements on a slice parallel to the *xz*-plane.

13. Experimental Setup

In cooperation of the Fraunhofer Institute for Information and Data Processing IITB and the Chair of Interactive Real-Time Systems of the Universität Karlsruhe, a sensor head has been developed consisting of an LC display acting as pattern generator and one or two cameras, see Fig. 10b. The compact design ensures that a rigid sensor head is obtained that maintains its geometric calibration over a longer period. To reduce the need of transferring a large amount of data image data for the pattern generator and recorded images from the cameras which would induce the need for precautionary measures regarding EMC (electromagnetic compatibility), a computer has been included in the sensor head which controls and synchronizes the pattern generation and the image acquisition. In addition, this computer performs preprocessing of the image data and decodes the image sequence. That way, only few data have to be transferred from this computer, keeping the required bandwidth from and to the sensor head tolerable.

The sensor head is mounted on an industrial robot which provides a six dimensional positioning of the sensor head, see Fig. 10a. The high stiffness of the industrial robot together with the used coding based on phase shifting ensures that no relevant vibrations of the sensor head occur.

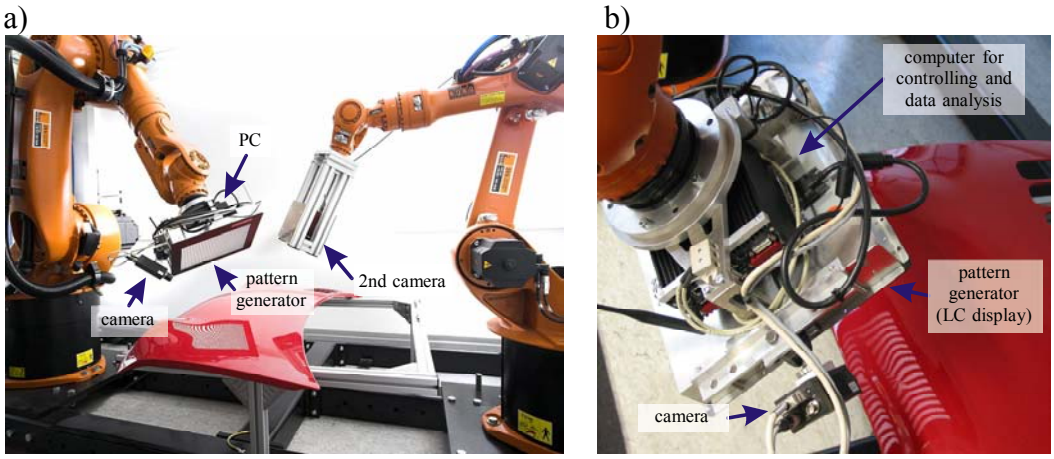

Fig. 10. Experimental setup: a) general view, b) sensor head.

In order to inspect the surface of large objects like *e.g.* car bodies, the surface is divided into regions which can be inspected individually from a single position of the sensor head. At each predefined position of the sensor head, an image series depicting the reflection of the code sequence on the pattern generator is taken and processed.

In addition to a full coverage of the surface to be inspected, the division of the surface into smaller overlapping regions offers the possibility to regularize the deflectometric reconstruction problem by means of a stereo approach in the overlapping areas, see Section 4.7. In order to use other regularization methods for a quantitative surface reconstruction, a second industrial robot is available that can be used for positioning *e.g.* another camera or an additional (laser) light source.

14. Conclusions

In this contribution, deflectometry has been introduced as a promising inspection principle for the industrial inspection of specular and partially specular surfaces. The opportunity to

evaluate deflectometric observations in order to generate a quantitative reconstruction together with the alternative of assessing geometric features offers the possibility to tailored inspection systems. However, deflectometry still imposes challenges in the practical application of the mathematical theory and is still a developing area in metrology. We have shown that by using industrial robots, a highly flexible deflectometric inspection setup is established which can be applied to a broad variety of surfaces. Further areas of improvements lie especially in the area of customized illumination and imaging setups for specialized production.

References

[1] F.E. Nicodemus, J.C. Richmond, J.J. Hsia, I.W. Ginsberg, T. Limperis: *Geometrical Considerations and Nomenclature for Reflectance*. NBS Monograph 160, National Bureau of Standards, U.S. Department of Commerce, Washington, DC, 1977.

[2] F. Remondino: "From point cloud to surface: the modeling and visualization problem". *International Archives of Photogrammetry, Remote Sensing and Spatial Information Sciences*, vol. XXXIV-5/W10, 2003.

[3] H. Hoppe: *Surface reconstruction from unorganized points. PhD thesis*. Dept. of Computer Science and Engineering, University of Washington, 1994.

[4] B.T. Phong: "Illumination for computer generated pictures". *Communications of the ACM* , vol. 18, no. 6, 1975, pp. 311-317.

[5] O. Kafri, A. Livnat: "Reflective surface analysis using moiré deflectometry". *Applied Optics,* vol. 20, no. 18, 1981, pp. 3098-3100.

[6] K. Ikeuchi: "Determining surface orientations of specular surfaces by using the photometric stereo method". *IEEE Transactions on Pattern Analysis and Machine Intelligence,* vol. 3, no. 6, 1981, pp. 661-669.

[7] R. Ritter, R. Hahn: "Contribution to analysis of the reflection grating method". *Optics and Lasers in Engineering,* vol. 4, no. 1, 1983, pp. 13-24.

[8] A. Sanderson, L. Weiss, S. Nayar: "Structured highlight inspection of specular surfaces". *IEEE Transactions on Pattern Analysis and Machine Intelligence,* vol. 10, no. 1, 1988, pp. 44-55.

[9] J. Balzer: *Regularisierung des Deflektometrieproblems – Grundlagen und Anwendung*. *PhD thesis*. Universität Karlsruhe, Universitätsverlag Karlsruhe, 2008.

[10] S. Kammel: *Deflektometrische Untersuchung spiegelnd reflektierender Freiformflächen. PhD thesis*. Universität Karlsruhe, Universitätsverlag Karlsruhe, 2004.

[11] D. Pérard: *Automated visual inspection of specular surfaces with structured-lighting reflection techniques*. *PhD thesis*. Universität Karlsruhe, VDI-Verlag, Düsseldorf, 2001.

[12] S.A. Shafer: "Using color to separate reflection components". *Color Research & Application,* vol. 10, no. 4, 1985, pp. 210-218.

[13] E.V. Verband der Automobilindustrie: *Dekorative Oberflächen von Anbau- und Funktionsteilen im Außen- und Innenbereich von Automobilen – VDA Band 16*, 2008.

[14] R. Chellappa, R.L. Kashyap: "Texture synthesis using 2-d noncausal autoregressive models". *IEEE Transactions on Speech and Signal Processing,* vol. 33, no. 1, pp. 194-203, 1985.

[15] C.W. Therrien, T.F. Quatieri, D.E. Dudgeon: "Statistical model-based algorithms for image analysis". *Proceedings of the IEEE,* vol. 74, no. 4, 1986.

[16] M. Topi, O. Timo, P. Matti, S. Maricor: "Robust texture classification by subsets of local binary patterns". *Proceedings of the ICPR 2000*, 2000, pp. 3947-3950.

[17] R.M. Haralick, K. Shanmugan, I. Dinstein: "Textural features for image classification". *IEEE Transactions on Systems, Man, and Cybernetics,* vol. 3, no. 6, 1973, pp. 610-621.

[18] A.E. Johnson, M. Hebert: "Using spin images for efficient object recognition in cluttered 3d scenes". *IEEE Transactions on Pattern Analysis and Machine Intelligence,* vol. 21, no. 5, 1999, pp. 433-449.

[19] J.H. Massig: “Deformation measurement on specular surfaces by simple means”. *Optical Engineering,* vol. 40, no. 10, 2001, pp. 2315-2318.

[20] S. Werling, J. Balzer, J. Beyerer: “Initial value estimation for robust deflectometric reconstruction”. *Proceedings of 8th International Conference on Optical 3-D Measurement Techniques*, no. 2, 2007.

[21] R.T. Frankot, R. Chellappa: “A method for enforcing integrability in shape from shading algorithms”. *IEEE Transactions on Pattern Analysis and Machine Intelligence,* vol. 10, no. 4, 1988, pp. 439-451.

[22] D. Terzopoulos: “The computation of visible-surface representations”. *IEEE Transactions on Pattern Analysis and Machine Intelligence,* vol. 10, no. 4, 1988, pp. 417-438.

[23] B. Karaçali, W. Snyder: “Reconstructing discontinuous surfaces from a given gradient field using partial integrability”. *Computer Vision and Image Understanding,* vol. 92, no. 1, 2003, pp. 78-111.

[24] B. Karaçali, W. Snyder: “Noise reduction in surface reconstruction from a given gradient field”. *Int. J. Comput. Vision,* vol. 60, no. 1, 2004, pp. 25-44.

[25] R. Kickingereder, K. Donner: “Stereo vision on specular surfaces”. *Proceedings of IASTED Conference on Visualization, Imaging, and Image Processing*, 2004, pp. 335-339.

[26] S. Ettl, J. Kaminski, E. Olesch, H. Strauß, G. Häusler: “Fast and robust 3d shape reconstruction from gradient data”. *DGaO Proceedings*, 2007.

[27] S. Ettl, J. Kaminski, M.C. Knauer, G. Häusler: “Shape reconstruction from gradient data”. *Applied Optics,* vol. 47, no. 12, 2008, pp. 2091-2097.

[28] J. Ho, J. Lim, M.H. Yang, D. Kriegman: “Integrating surface normal vectors using fast marching method”. *Lecture Notes in Computer Science*, 2006.

[29] P. Kovesi: “Shapelets correlated with surface normals produce surfaces”. *ICCV ’05: Proceedings of the Tenth IEEE International Conference on Computer Vision*, IEEE Computer Society, 2005.

[30] P. Bochev, R.B. Lehoucq: “On the finite element solution of the pure neumann problem”. *SIAM Rev.,* no. 47, 2005, pp. 50-66.

[31] S. Savarese, M. Chen, P. Perona: “Local shape from mirror reflections”. *International Journal of Computer Vision,* vol. 64, no. 1, 2005, pp. 31-67.

[32] A. Zisserman, P. Giblin, A. Blake: “The information available to a moving observer from specularities”. *Image Vision Comput.,* vol. 7, no. 1, 1989, pp. 38-42.

[33] S. Roth, M. Black: “Specular flow and the recovery of surface structure”. *Proceedings of IEEE Conference on Computer Vision and Pattern Recognition,* no. 2, 2006, pp. 1869-1876.

[34] J. Lellmann, J. Balzer, A. Rieder, J. Beyerer: “Shape from specular reflection and optical flow”. *International Journal of Computer Vision,* vol. 80, no. 2, 2008, pp. 226-241.

[35] S. Rahmann, N. Canterakis: “Reconstruction of specular surfaces using polarization imaging”. *Proceedings of the IEEE Computer Society Conference on Computer Vision and Pattern Recognition (CVPR)*, no. 1, 2001, pp. 149-155.

[36] L.B. Wolff: “Surface orientation from two camera stereo with polarizers”. *Proc. SPIE, Optics, Illumination, and Sensing for Machine Vision IV,* vol. 1194, 1989, pp. 287-297.

[37] G.A. Atkinson: *Surface Shape and Reflectance Analysis Using Polarisation*. *PhD thesis*. University of York, 2007.

[38] Z. Wang, S. Inokuchi: “Determining shape of specular surfaces”. *The 8th Scandinavian Conference on Image Analysis*, 1993, pp. 1187-1194.

[39] T. Bonfort, P. Sturm: “Voxel carving for specular surfaces” *Proc. ICCV*, 2003, pp. 591-596.

[40] M. Knauer, J. Kaminski, G. Häusler: “Phase measuring deflectometry: a new approch to measure specular free-form surfaces”. *Optical Metrology in Production Engineering*, *Proc. SPIE,* 5457, 2004, pp. 366-376.

[41] M. Petz, R. Tutsch: “Reflection grating photogrammetry: a technique for absolute shape measurement of specular free-form surfaces”. *Proceedings of the SPIE Conference on Optical Manufacturing and Testing VI*, 2005, pp. 58691D1 – 58691D12.

[42] J. Balzer: “Über die Eindeutigkeit der stereo-regularisierten deflektometrischen Oberflächenrekonstruktion”. *Tagungsband Bildverarbeitung in der Mess- und Automatisierungstechnik, Regensburg*, 2007.

[43] J. Balzer, S. Werling, J. Beyerer: “Regularization of the deflectometry problem using shading data”. *Proceedings of the SPIE Optics East*, 2006.